The 2012 World Congress on
Advances in Civil, Environmental, and Materials Research (ACEM' 12)
Seoul, Korea, August 26-30, 2012

Suction Controlled Saturation Processes of Buffer Material in a Deep Geological Repository

*Wei-Hsing Huang[1)] and Yi-Fang Chuang[2)]

[1), 2)] *Department of Civil Engineering, National Central Univ., Jhongli 32001, Taiwan*
[1)] *t321655@ncu.edu.tw*

ABSTRACT

Buffer material, acting as an engineered clay barrier, plays a major role for the isolation of radioactive wastes in a deep geological repository. This paper investigates the saturation behavior in the near field of a disposal site, with emphasis on the variation of soil suction with the temperature and degree of saturation. A detailed laboratory program was implemented to obtain soil suction characteristics curve at various temperatures using vapor equilibrium technique. It was found that soil suction decreases as temperature increases, resulting in a reduction in water retention capability. A finite element model simulating the hydro-mechanical behavior in the resaturation processes of the buffer material was developed. The model was validated through a comparison with the water uptake test results obtained at elevated temperatures.

1. INTRODUCTION

Clay-based materials serve as buffer material in an engineered barrier system for isolation of high-level radioactive wastes in a repository. The safety of a deep geological repository depends upon the stability of engineering barriers. Being a major component in the barrier system, buffer material is expected to create an impermeable zone around the high level waste canisters. Compacted bentonites have been considered by many countries as the prime candidate for buffer material due to their sealing capacity.

In the current proposal for deep geological disposal of the high-level wastes (HLW) in Taiwan, compacted bentonite is used to contain the metallic waste canisters and separate the waste from the host rock and backfill materials. The major roles of the buffer material are to reduce the groundwater flow, to protect the overpack from degradation and to minimize the migration of radionuclides.

In a HLW repository, after emplacement of the buffer material, groundwater begins to be taken from the surrounding rock by the buffer and the buffer becomes

---

[1)] Professor
[2)] Graduate Student

saturated gradually. Groundwater intrusion is taken as an important scenario in the performance assessment of a geological repository. The resaturation of the buffer is considered a hydro-process occurring at elevated temperatures in the near-field of a repository. Factors affecting this process include the far-field supply of water, the hydraulic conductivity of the rock, the piezometric conditions, and the initial degree of saturation of the buffer (SKB, 1999).

Groundwater flow through buffer is coupled with the mechanical changes induced by in-situ stresses and the thermal loading resulting from heat generated by the radioactive waste. It is important to model these effects carefully to provide a full picture of the flow through the barrier. Due to the long duration of the process and the scale of the medium considered, the only way to quantify these processes experimentally is to implement on a reduced scale. The measurements made in such experiments would make it possible to refine the numerical models and validate the models for subsequent use in simulating real disposal situation.

This paper addresses the hydro-thermal features that might affect the flow of groundwater in the near-field of a waste repository. A locally available clay material is characterized for its temperature-dependent suction in unsaturated states such that coupling of the hydro- and thermo- effects of the clay barrier can be evaluated. With emphasis on the soil-water characteristic curve of unsaturated soil behavior of the bentonite, simulations of the resaturation processes of buffer material upon groundwater intrusion in the near-field were carried out numerically in this study.

2. MATERIALS AND METHODS

The potential buffer material used in this study is a commercial clay, originated from the east coast of Taiwan, known as Zhisin clay. The CEC of Zhisin clay was found to be 69.5 cmol/kg, as calculated by summing up the individual calcium (38.7 cmol/kg), sodium (23.1 cmol/kg), potassium (1.4 cmol/kg), and magnesium ions (6.8 cmol/kg) present. Experimental results indicated that the dominant exchangeable cation for Zhisin clay is Ca^{2+}. Thus, Zhisin clay is considered as a Ca-bentonite.

Consistency limits, grain size distribution, and specific gravity of Zhisin clay were determined in accordance with ASTM D 4318, D 422, and D 854, respectively. Table 1 presents the geotechnical properties of Zhisin clay. It is noted that the plasticity index of Zhisin clay (49%) is much lower than that of other bentonites for similar applications, such as Kunigel VI clay for Japan (395%), Avonseal clay for Canada (285%), and MX-80 bentonite for Sweden (330%). Apparently, this is because Zhisin clay is a Ca-type bentonite, while the other bentonites are of the Na-type (Chen and Huang, 2004).

Table 1 Geotechnical properties of Zhisin clay

Grain size (%)			Consistency limits (%)		
sand	silt	clay	LL	PL	PI
28	46	26	67	18	49

Also used in this study is another bentonite originated from Black Hills, Wyoming, designated as BH bentonite. This was selected as a reference material as its material characteristics are very similar to MX-80 bentonite. For the very high suctions inherent to bentonite materials, the controlled relative humidity technique was employed to determine the soil suction of bentonite at various temperatures. To control the relative humidity of the air surrounding the sample, compacted Zhisin clays were placed in a desiccator containing an aqueous solution of a given chemical compound. And all desiccators were then placed in a temperature control cabin. According to the physical-chemical properties of the compound, a given relative humidity is imposed within the desiccator. Water exchanges occur by vapor transfer between the solution and the sample, and a given suction is applied to the sample when vapor equilibrium is reached.

The relationship between the soil total suction and the relative humidity of the pore water vapor is described by Kelvin's equation, as follows:

$$u_a - u_w = \frac{RT}{V}\ln\left(\frac{P}{P_0}\right) \tag{1}$$

where u_a and u_w are the air and water pressures (kPa), R = universal gas constant [8.31432 J/(mol K)], T = absolute temperature (K), V = molar volume of water (m^3/kmol), P/P_0 = relative humidity, P = partial pressure of pore water vapor (kPa) and P_0 = saturation pressure of water vapor over a flat surface of pure water at the same temperature (kPa).

3. SOIL WATER CHARACTERISTICS CURVE

Using several selected salts for control of the relative humidity at various levels, the suction of the Zhisin clay sample as a function of water content or degree of saturation, termed soil-water characteristic curve, can be determined. Figs. 1 and 2 show the SWCC of the 2 barrier materials at various elevated temperatures, respectively. It should be noted that the uncertainty of control relative humidity technique poses a limitation for determining suctions < 10 MPa. To extend the SWCC and cover the entire suction range, the equations proposed by Fredlund and Xing (1994a) was used. The Fredlund and Xing model for SWCC has the following form:

$$S = C(\psi)\frac{1}{\left[\ln\left[e+\left(\frac{\psi}{\psi_i}\right)^n\right]\right]^m} \tag{2}$$

where S is the degree of saturation, ψ is soil suction, ψ_i is the air-entry suction value of the soil, n and m are curve fitting parameters, and $C(\psi)$ is a correction function defined as

$$C(\psi) = \frac{\ln(1+\psi/\psi_r)}{\ln\left[1+\left(10^6/\psi_r\right)\right]} \tag{3}$$

where ψ_r is a constant related the residual suction corresponding to the residual degree of saturation. Experimental data have previously shown that the suction of a soil reaches a maximum value of approximately 10^6 kPa at zero degree of saturation.

Figs. 1 and 2 illustrate the experimental data obtained from controlled relative humidity technique conducted at elevated temperatures of 25℃, 40℃, and 60℃. Eq. (2) was used to establish the SWCC over the entire range of degree of saturation, with the curve-fitting parameters shown in Table 2.

It is noted from Figs. 1 and 2 that the suctions of BH bentonite are higher than that of Zhisin clay, due to the fact that BH bentonite has a higher plasticity. Suctions of the 2 bentonite are shown to vary slightly with temperature. In general, soil suctions decrease with increasing temperature.

Table 2 Curve-fitting parameters using Eq. (2)

Parameter	BH bentonite			Zhisin clay		
	25℃	40℃	60℃	25℃	40℃	60℃
ψ_i (kPa)	3900	2900	2300	800	320	300
n	0.70	0.76	0.76	0.55	0.55	0.55
m	1.00	1.02	1.02	1.5	1.5	1.5

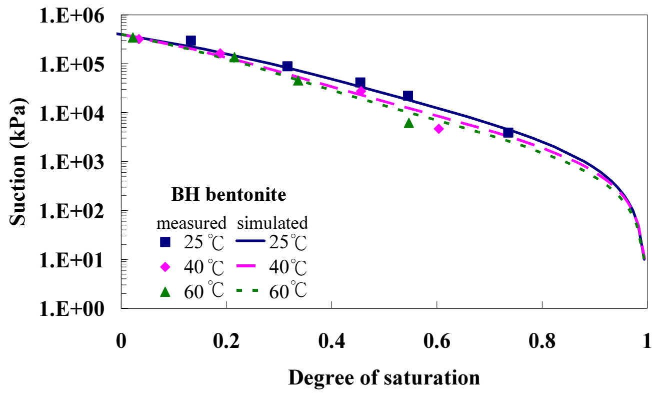

Fig.1 SWCC of BH bentonite at various temperatures

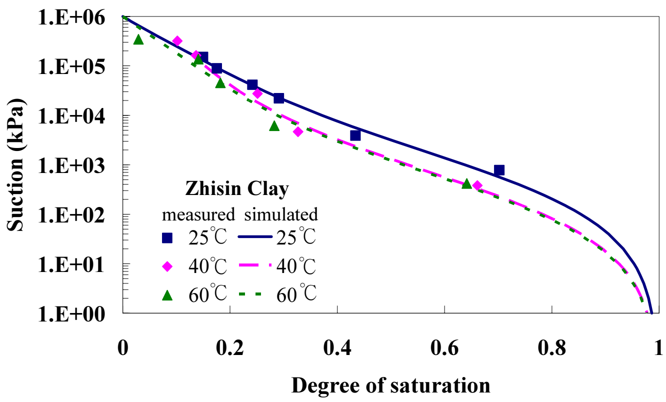

Fig. 2 SWCC of Zhisin clay at various temperatures

The hydraulic conductivity of saturated Zhisin clay was determined by applying high hydraulic pressures to a specimen column of 70 mm in height. Figs. 3 and 4 show the relationships between temperature and hydraulic conductivity of BH bentonite and Zhisin clay, respectively, compacted at various dry densities/void ratios. It is observed that the hydraulic conductivity of Zhisin clay is very sensitive to temperature, and increases with the increase in temperature.

The barrier material is in unsaturated conditions at the beginning of the resaturation processes. The hydraulic conductivity of an unsaturated soil depends on the volumetric water content, which, in turn, depends on the soil suction, ψ. Thus, it can be predicted from the soil-water characteristic curve. Based on the fact that both the hydraulic conductivity and the SWCC are primarily determined by the pore size distribution of the soil under consideration, statistical models can be used to predict the hydraulic conductivity when the saturated hydraulic conductivity, k_s, and the SWCC are available. The calculation of the hydraulic conductivity $k(\theta_i)$ of unsaturated soil at a specific water content θ_i involves the summation of the suction values that correspond to the water content at and belowθ_i. The relative hydraulic conductivity $k_r(\theta_i)$, based on the saturated hydraulic conductivity k_s, is necessary to provide a more accurate fit for the unsaturated hydraulic conductivity. Eq. (4) shows the prediction equation developed by Kunze et al. (1968).

$$k_r(\theta_i) = \left(\frac{\theta_i}{\theta_s}\right) \frac{\sum_{j=i}^{m}\left[\frac{(2j+1-2i)}{\psi_j^2}\right]}{\sum_{j=1}^{m}\left[\frac{(2j-1)}{\psi_j^2}\right]} \tag{4}$$

where $k_r(\theta_i)$ is the relative hydraulic conductivity at water content θ_i, k_s is the saturated hydraulic conductivity, m is the number of increments of θ subdivided on the characteristic curve, ψ is the suction head at the midpoint of each water content increment, and i and j are summation indices.

The calculations are performed by dividing the relation between volumetric water content and suction into m equal water-content increments. With the soil-water characteristic curve given in Fig. 1, the relative hydraulic conductivity k_r of unsaturated Zhisin clay can be derived using Eq. (4). Fig. 5 shows the relationships between the calculated relative hydraulic conductivity and the degree of saturation for the 2 bentonites studied. It can be observed from Fig. 5 that the hydraulic conductivity of a single soil ranges over 8 orders of magnitude when considering the soil from a dry state to a saturated condition.

4. WATER UPTAKE TESTS

Test specimens in their air-dried conditions were compacted to specified dry densities with a dimension of 60 mm in diameter and 50 mm in height. A schematic of the test apparatus is shown in Fig. 6. The apparatus was placed in a water bath maintained at the desired temperatures. The base plate was made perforated to allow uptake of water from the bottom of the specimen. The specimen became saturated, from the lower portion tot the upper portion, gradually and sequentially.

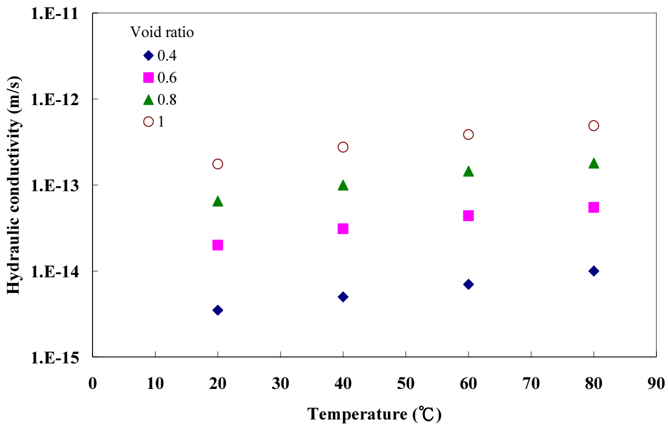

Fig. 3 Relationships between temperature and hydraulic conductivity of BH bentonite

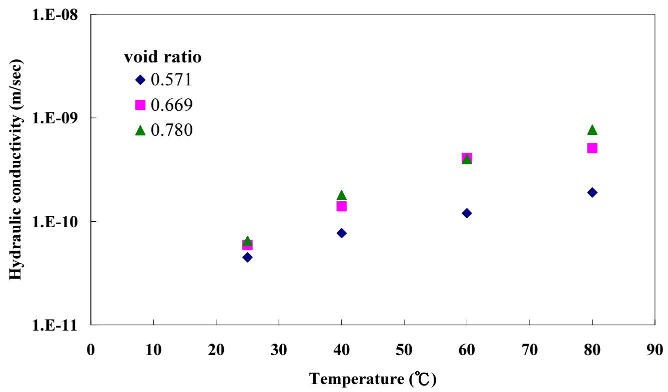

Fig. 4 Relationships between temperature and hydraulic conductivity of Zhisin clay

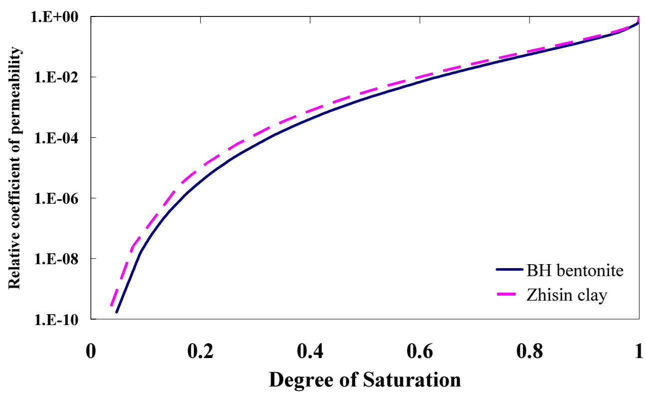

Fig. 5 Relationships between relative hydraulic conductivity and degree of saturation

The specimen was kept in the saturation process for a pre-determined duration of 1-day to 4 weeks. At the end of the duration, the specimen was extracted from the mold and sectioned into slices. Then the bentonite slices at different distance from the inlet were determined for their water content, such that the profile of degree of saturation along the distance from the inlet can be drawn. To account for the effects of

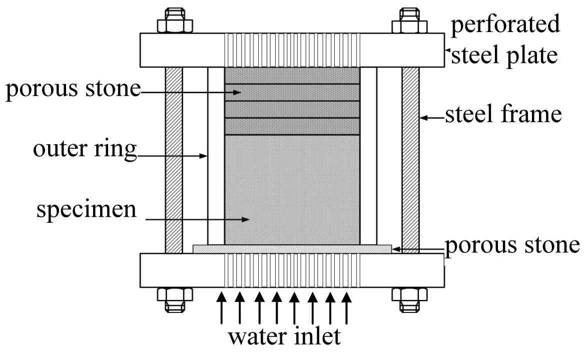

Fig. 6 Schematic of the water uptake test

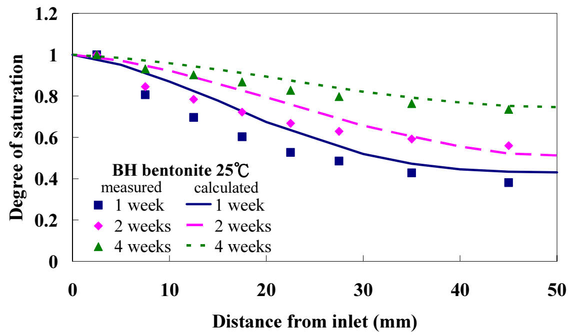

(a) 25℃

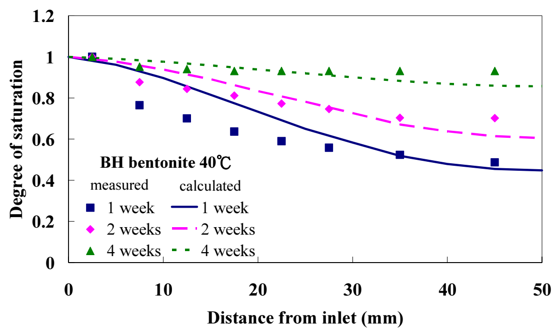

(b) 40℃

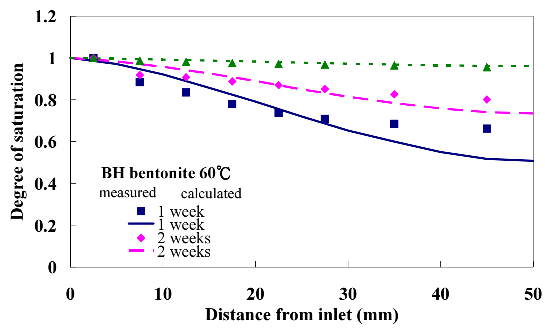

(c) 60℃

Fig. 7 Comparison between measured and calculated results for the water uptake test conducted on BH bentonite at different temperatures

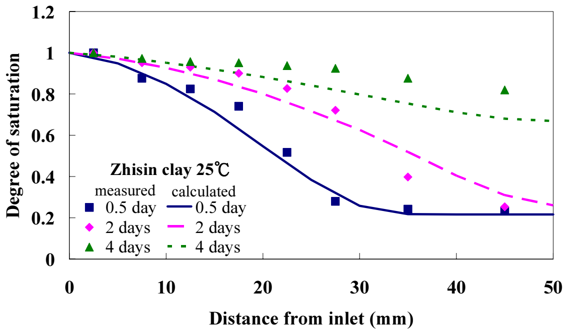

(a) 25℃

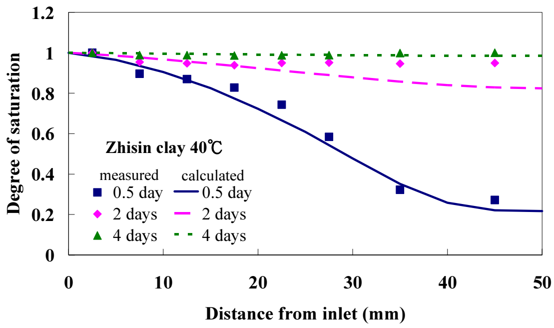

(b) 40℃

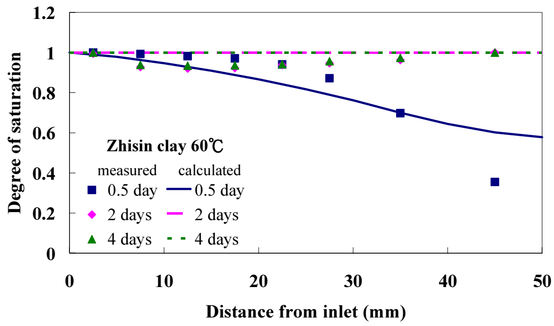

(c) 60℃

Fig. 8 Comparison between measured and calculated results for the water uptake test conducted on Zhisin clay at different temperatures

temperature on the saturation processes, the water uptake tests were conducted at 25℃, 40℃, and 60℃.

The water uptake experiment was simulated by use of the finite element code ABAQUS. Detailed information on the theoretical background and available models is documented in the ABAQUS manuals. The modeling techniques used in simulating the water uptake test were briefly described by Lu et al. (2006). The test was modeled by a 2×10 finite element mesh with a dimension of 5 mm by 25 mm.

The calculated degree of saturation profile at different times after water intake is compared to those obtained from the measurements in water uptake tests. Figs. 7 and 8 show the comparison between measured and calculated degree of saturation profiles for BH bentonite and Zhisin clay, respectively. The time listed in these figures represents the time period from the start of water intake to the moment that specimens were extracted from the mold and determined for water content. It is found that, for all the temperatures tested, the calculated degree of saturation profiles are close to that of the experimental data and both exhibit similar shape.

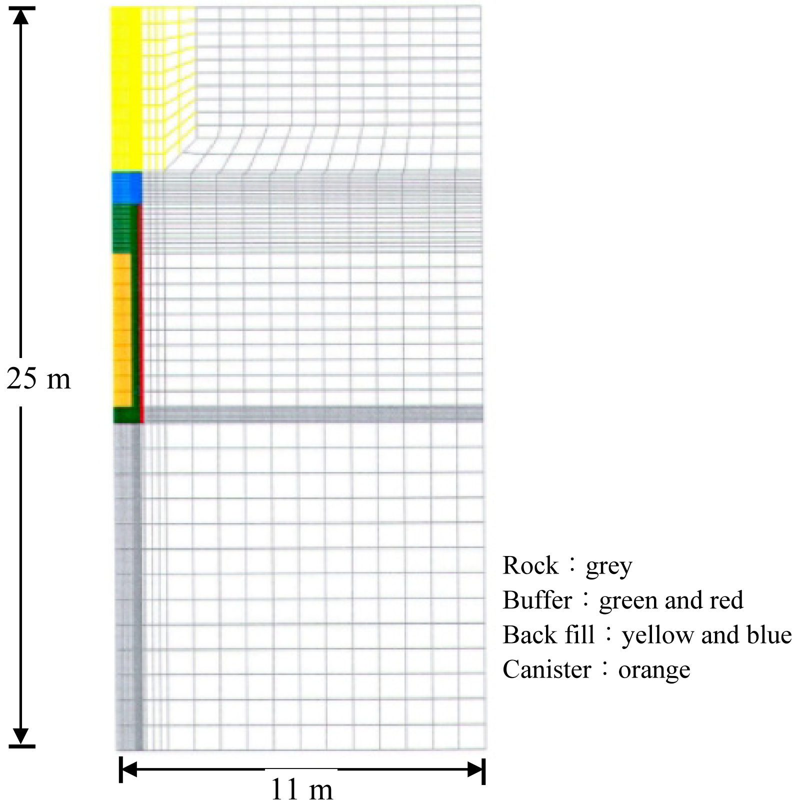

Fig. 9 Finite element mesh for the deposition hole

5. NUMERICAL SIMULATION

The numerical simulation of the resaturation processes in the vicinity of a deposition hole was carried out through iterations of thermal and hydro-mechanical calculations. Based on the simulation results from water uptake tests, the saturation process of the buffer material in a deposition hole is simulated using a finite element model shown in Fig. 9, which is similar to the model used by Börgesson (1999).

The simulation started with a heat transfer calculation assuming a canister body heat flux of 449.289 W/m^3 and a decay heat function shown in Fig. 10. Then the hydro-mechanical calculation was performed by incorporating the suction and hydraulic conductivity of unsaturated buffer material. In addition, thermal properties (Fig. 11) of the buffer material as a function of temperature were introduced.

Fig. 12 shows the effect of incorporating the hydraulic features into the simulation calculation on the temperature distribution in the buffer material (BH bentonite) at the end of the resaturation process. It is found that the, due to the variation in suction and thermal conductivity with temperature of buffer material, the calculated temperature shows a reduction as a result of introducing the hydro-properties in the calculations. Fig. 13 exhibits a similar trend derived from from Zhisin clay, as compared to that of BH bentonite.

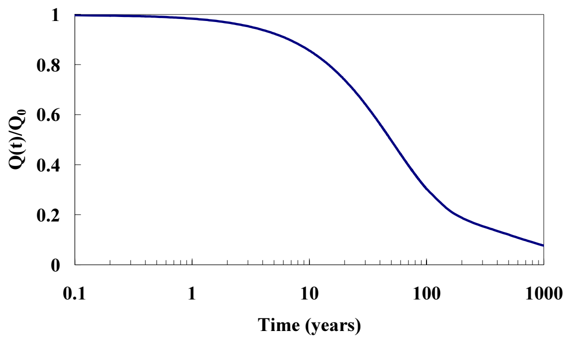

Fig. 10 Decay heat function of canister

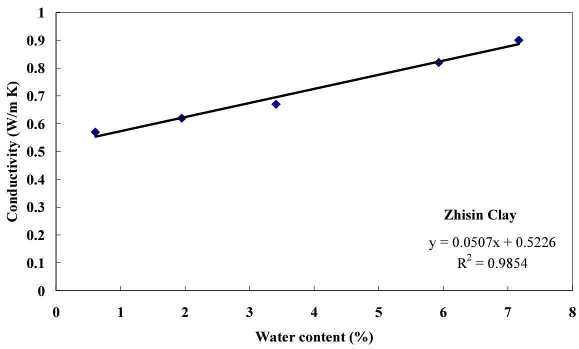

Fig. 11 Relationship between thermal conductivity and water content of Zhisin clay

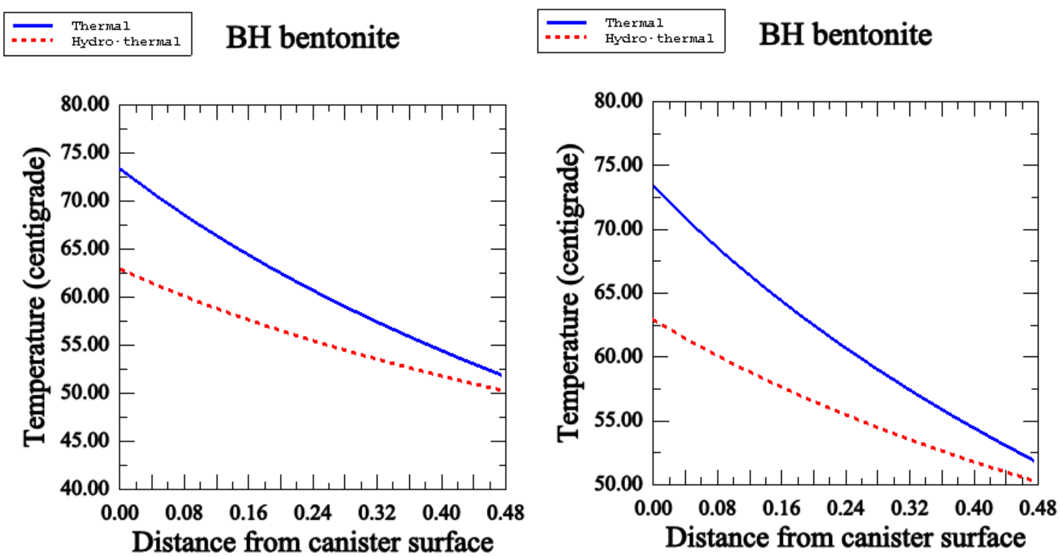

Fig. 12 Comparison of temperature profiles along the thickness of buffer material between thermal-only and thermal-hydro simulation (BH bentonite)

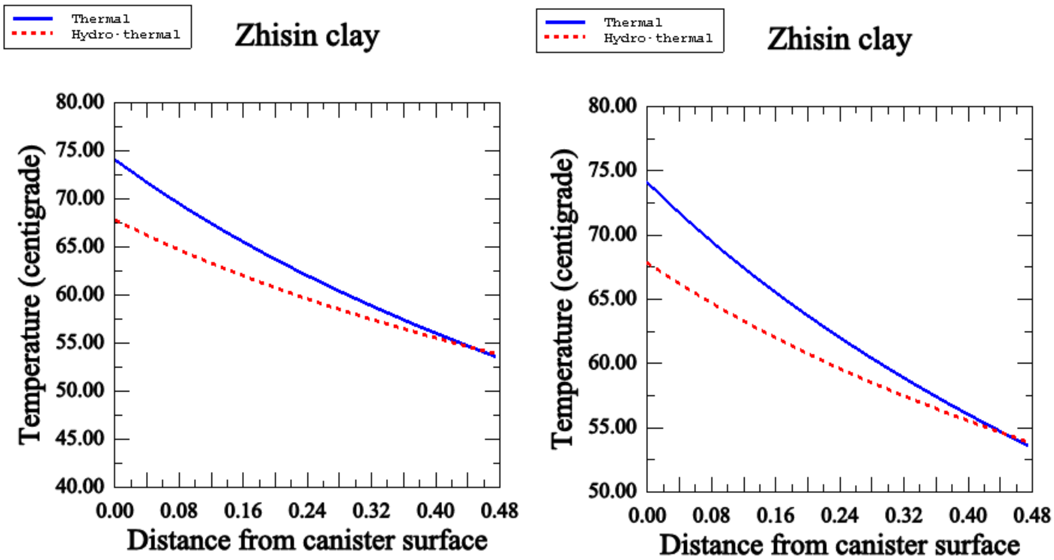

Fig. 13 Comparison of temperature profiles along the thickness of buffer material between thermal-only and thermal-hydro simulation (Zhisin clay)

6. CONCLUSIONS

This study simulates the resaturation process of buffer material in the deposition hole of a radioactive waste repository using both experimental method and numerical modeling techniques. Experimental works on Zhisin clay provided measurements on the suctions and hydraulic conductivity of buffer material in unsaturated conditions, such that finite element model can be developed to simulate the resaturation process with consideration on hydraulic characteristics of the buffer material as a function of degree of saturation and temperature.

Experimental results on potential buffer materials show that the suctions of buffer material are of great importance to the hydro-behavior of bentonite. In the simulation of resaturation process of buffer material, it is necessary to take the hydraulic characteristics of unsaturated soils into account. The coupling effects of thermal, hydro, and mechanical processes play a major role in the resaturation behavior of the buffer. Future study is necessary to incorporate the the coupling effects for the simulation of moisture and temperature distribution in the near-field of a geological repository.

7. REFERENCES

Fredlund, D. G., and Xing, A. (1994a). “Equations for the soil-water characteristic curve,” *Canadian Geotechnical Journal*, Vol. 31, 521-532.

Fredlund, D. G., Xing, A., and Huang S. (1994b) “Predicting the permeability function for unsaturated soil using the soil-water characteristic curve.” *Canadian Geotechnical Journal*, Vol. 31, 533-546.